

Supplementary Information

Dual heterojunctions-based Au@TiO₂ photoelectrode exhibiting efficient charge separation for enhanced removal of organic dye under visible light

Pan Zhang,^a Yuzhou Jin,^a Mingfang Li,^a Xuejiang Wang,^b Ya-nan Zhang^{*a}

a. School of Chemical Science and Engineering, Shanghai Key Lab of Chemical Assessment and Sustainability, Key Laboratory of Yangtze River Water Environment, Tongji University, Shanghai 200092, People's Republic of China.

b. College of Environmental Science and Engineering, Shanghai Institute of Pollution Control and Ecological Security, Tongji University, Shanghai 200092, PR China

Email: yananzhang@tongji.edu.cn

Table S1 Parameters of photoelectrochemical measurements of A-FH TiO₂/Ti, 1%Au@A-FH TiO₂/Ti, 2%Au@A-FH TiO₂/Ti and 4%Au@A-FH TiO₂/Ti.

Photoelectrode	Photocurrent (10 ⁻⁵ A cm ⁻²)	Resistance value (10 ³ Ω)	Donor density (N _D :×10 ²⁰ cm ⁻³)
A-FH TiO ₂ /Ti	0.70	14	1.27
1%Au@A-FH TiO ₂ /Ti	0.75	12	1.58
2%Au@A-FH TiO ₂ /Ti	1.15	5	2.67
4%Au@A-FH TiO ₂ /Ti	0.90	7.5	2.43

Table S2 The bend enrgy (BE) position and raw area of A-FH TiO₂/Ti and Au@A-FH TiO₂/Ti.

Photoelectrode	Peak	Split Peak	Position	Raw Area
			BE (eV)	(cps eV)
A-FH TiO ₂ /Ti	Ti 2p	Ti ⁴⁺ 2p _{3/2}	458.7	10837.9
		Ti ⁴⁺ 2p _{1/2}	464.4	
	O 1s	Ti-O-Ti	529.9	19262.1
		Ti-O-H	532.7	
Au@A-FH TiO ₂ /Ti	Ti 2p	Ti ⁴⁺ 2p _{3/2}	458.9	7241.4
		Ti ⁴⁺ 2p _{1/2}	464.6	
	O 1s	Ti-O-Ti	530.2	10957.2
		Ti-O-H	533.0	
	Au 4f	Au ⁰ 4f _{7/2}	83.0	3173.9
		Au ⁰ 4f _{5/2}	86.8	

Table S3 The light absorption (η_{abs}), charge separation (η_{sep}), and injection efficiency (η_{inj}) of all photoelectrodes.

Photoelectrode	η_{abs}	η_{sep}	η_{inj}
Au@A-TiO ₂ /Ti	32.6 %	1.1 %	7.9 %
A-FH TiO ₂ /Ti	45.2 %	1.3 %	20.2 %
Au@A-FH TiO ₂ /Ti	54.5 %	3.9 %	40.8 %

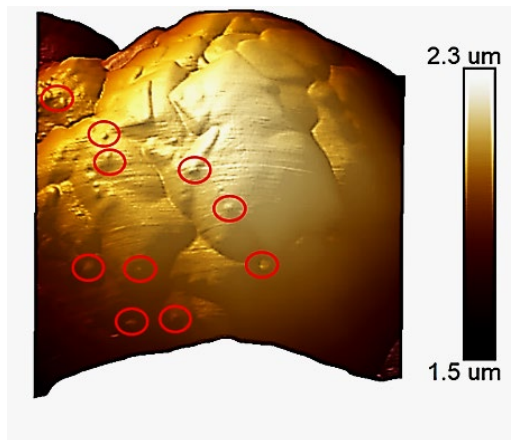


Fig. S1 AFM 3D diagram of Au@A-FH TiO₂/Ti.

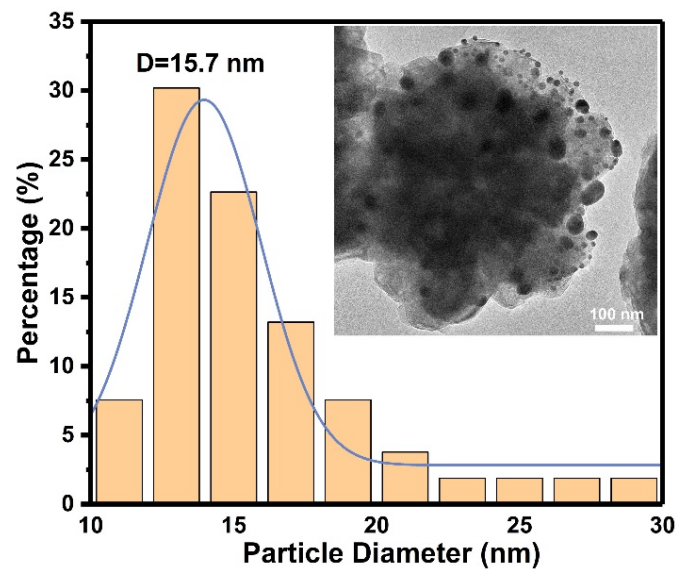


Fig. S2 Au particle size distribution of 2%Au@A-FH TiO₂/Ti.

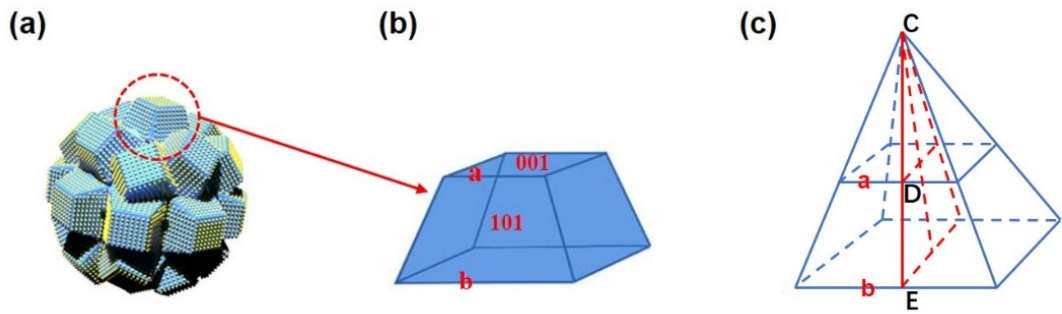


Fig. S3 Model schematic of (a) nanoflower-like TiO_2 microspheres, (b) truncated tetragonal pyramid and (c) truncated pyramid.

The exposure percentage of $\{001\}$ facet is about 70% calculated by the formula below:

$$\begin{aligned}
 S_{\{001\}\text{exp}} (\%) &= S_{\{001\}} / (S_{\{101\}} + S_{\{001\}}) \\
 &= 2a^2 / [2a^2 + 8 \times (0.5 CE \times b - 0.5 CD \times a)] \\
 &= \cos\theta / [\cos\theta + (a/b)^2 - 1]
 \end{aligned}$$

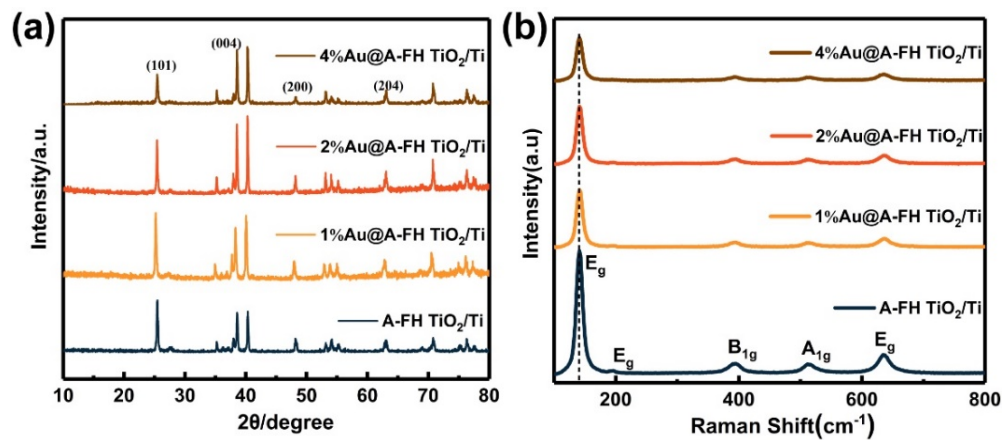


Fig. S4 The XRD patterns (a) and Raman spectra (b) of photoelectrodes.

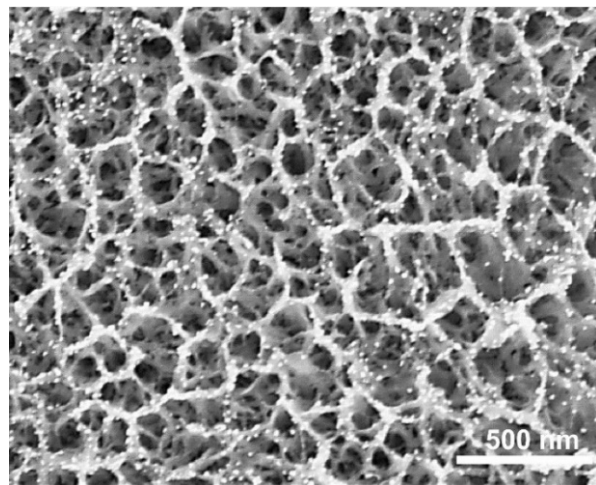


Fig. S5 SEM images of Au@A-TiO₂/Ti without specific crystal facet.

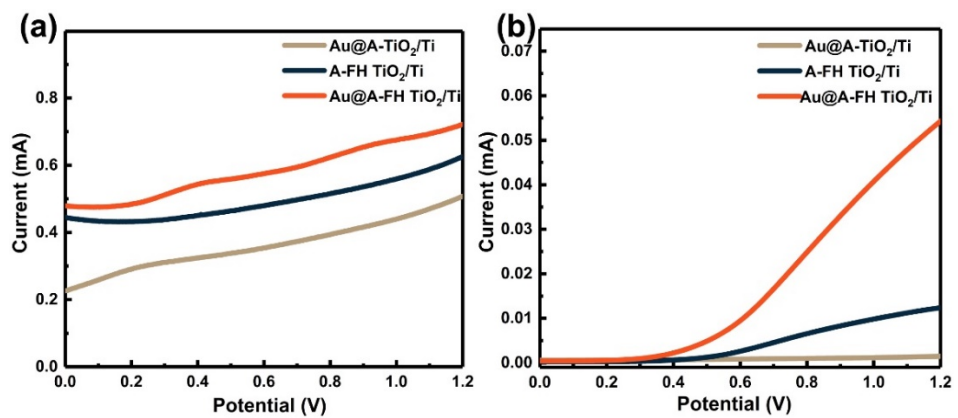


Fig. S6 LSV curves in $0.1 \text{ M Na}_2\text{SO}_4$ (a) and Na_2SO_3 (b) solution of three samples under AM1.5G illumination.

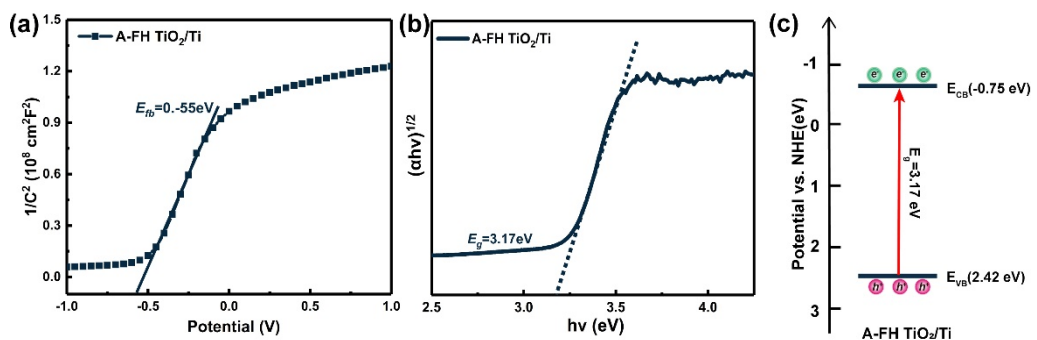


Fig. S7 The band structure diagram (c) calculated by band gap value (a) and flat band (b) of A-FH TiO_2/Ti .

The conduction band (E_{CB}) of TiO_2 is generally considered to be more negative by 0.2 eV relative to the flat band (E_{fb}).

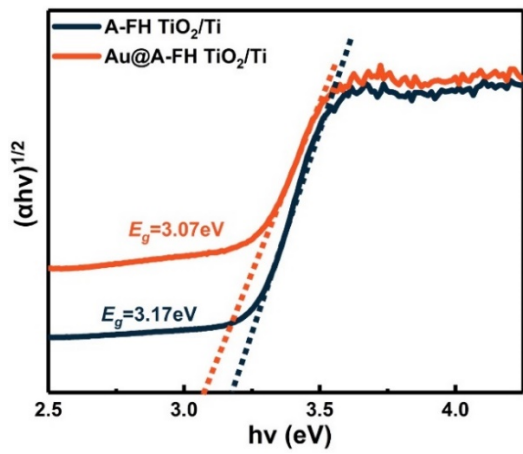


Fig. S8 Calculated band gap energy of A-FH TiO_2/Ti and Au@A-FH TiO_2/Ti .

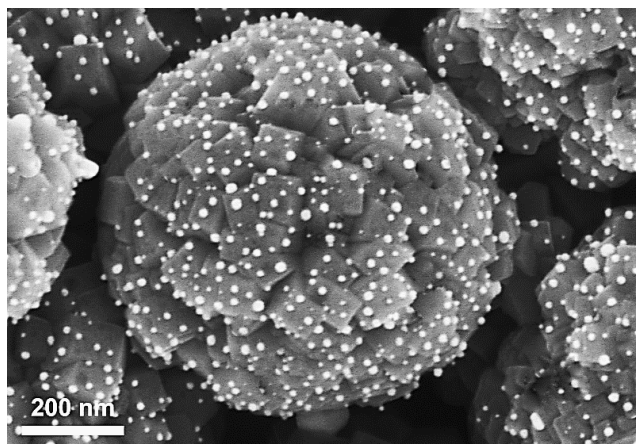


Fig. S9 The SEM images of Au@A-FH TiO₂/Ti after 5 cycles.

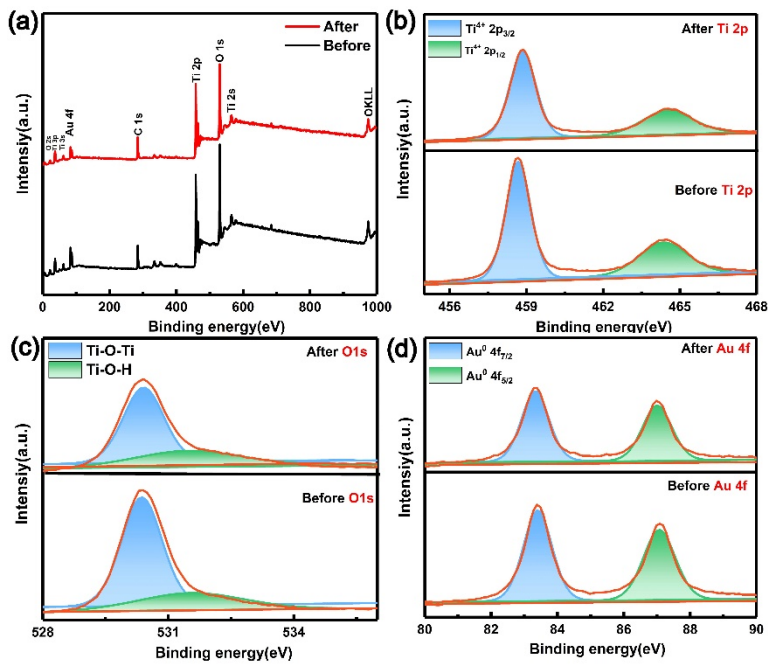


Fig. S10 The XPS spectra (a), Ti 2p (b), O 1s (c) and Au 4f (d) spectra of A-FH TiO_2/Ti and $\text{Au}@\text{A-FH TiO}_2/\text{Ti}$ after five cycles.

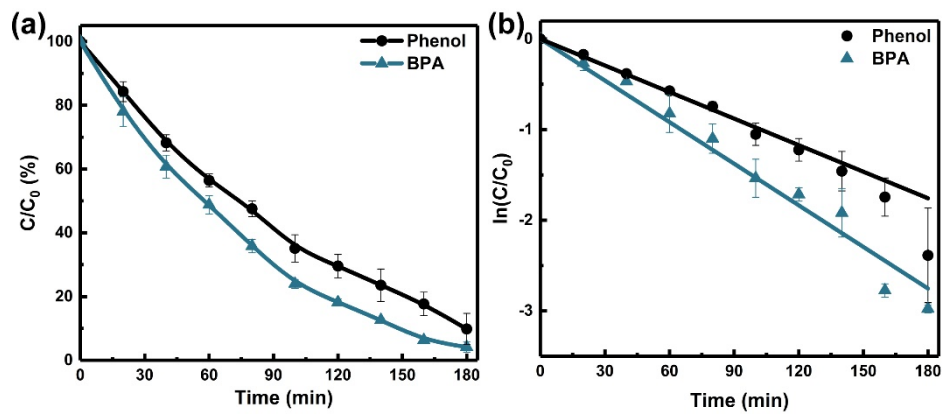


Fig. S11 The degradation and first order kinetic curves for phenol and Bisphenol A degradation